

ChartBlender: An Interactive System for Authoring and Synchronizing Visualization Charts in Video

Yi He, Yuqi Liu, Chenpu Li, Ruoyan Chen, Chuer Chen, Shengqi Dang, and Nan Cao



Abstract—Embedding data visualizations in video can enhance the communication of complex information. However, this process is often labor-intensive, requiring designers to adjust visualizations frame by frame manually. In this work, we present ChartBlender, a novel system that streamlines this process by enabling users to create data visualizations, embed them seamlessly into video scenes, and automatically synchronize them with both camera motion and moving objects. Particularly, ChartBlender incorporates a tracking algorithm that supports both object and camera tracking, ensuring robust alignment of visualizations with dynamic video content. To maintain visual clarity and aesthetic coherence, we also explore the design space of video-suited visualizations and develop a library of customizable templates optimized for video embedding. We evaluate ChartBlender through two controlled experiments and expert interviews with five domain experts. Results show that our system enables accurate synchronization and accelerates the production of data-driven videos.

Index Terms—data visualization, video editing, object tracking, camera tracking, interface, visual storytelling.

1 INTRODUCTION

EMBEDDING data visualizations into videos has emerged as a powerful method for conveying complex information [1]–[5]. Such a form of representation is increasingly used across various domains (e.g., sports, traffic, and journalism), allowing audiences to access supplementary information without being distracted from the primary video content [6]. Despite its potential, the process remains labor-intensive: achieving spatial and temporal synchronization between visualizations and video typically requires manual, frame-by-frame alignment. Even a 10-second visualization-embedded video may demand up to a full day of manual work from designers.

Motivated by a collaborative project with a major Chinese media organization to create a chart-embedded video, we conducted a comprehensive survey of existing tools and systems. On one end of the spectrum are professional tools like Adobe After Effects [7] and Blender [8]. While powerful, these tools rely on manual parameter tuning and lack intelligent assistance, making them difficult to use

efficiently. On the other end, recent advances in Augmented Reality (AR) and Virtual Reality (VR) have inspired research systems that allow casual users to overlay visualizations on videos for sharing quickly [9]. These systems prioritize ease of use and rapid output but are designed primarily for end users with simple needs. As a result, they fall short in supporting high-quality, professionally produced content. Specifically, they lack robust motion tracking for objects with diverse movement patterns, as well as precise control over visualization placement and editing capabilities essential for content creators and news organizations.

Therefore, there is a pressing need for an interactive authoring system supports flexible, efficient embedding of data visualizations into complex video scenes and ensures accurate motion synchronization throughout the video. However, to design such an effective system, three challenges need to be tackled: (1) track the motion of videos accounting for both moving objects in the scene and camera pose variations, to ensure consistent synchronization between visualizations and the video scene; (2) design generalized visualizations to support clear and informative presentation of data within dynamic video contexts; and (3) enable user-driven authoring and refinement of visualizations through simple and integrated interaction. Addressing these challenges is essential for the precise and seamless embedding of data visualizations into real-world videos.

To address these challenges, we introduce *ChartBlender*, a novel authoring system for embedding and automatically synchronizing data visualizations with video during playback. In particular, the user simply selects a target tracking point and a preferred tracking mode, and the system automatically generates the complete motion trajectory for visualization throughout the video. Users can edit the visualization at any time, including both its visual style and its 3D pose within the video scene. In this way, the system supports the human-machine collaboration to generate data-driven videos rapidly while ensuring the visualization appears visually coherent and seamlessly embedded into the video. The major contributions of the paper are as follows:

- **System.** We introduce *ChartBlender*, a novel authoring system that enables the authoring and automatic synchronization of data visualizations with video content. It features an interactive interface that supports the end-to-end creation of visualization-embedded videos

Yi He, Yuqi Liu, Chenpu Li, Ruoyan Chen, Chuer Chen, Shengqi Dang, and Nan Cao are with the Intelligent Big Data Visualization Lab, Tongji University. Email: {heyi_11, 2333349, 2251319, 2433555, chuerchen, dangsq123, nan.cao}@tongji.edu.cn.

Nan Cao is the corresponding author. Email: nan.cao@gmail.com

through an integrated authoring workflow.

- **Design Space.** We characterize the design space of visualizations suitable for video embedding. Specifically, we identify two primary motion modes, **camera tracking** and **object tracking**, and identify five commonly used chart types. Based on this analysis, we develop a library of generalized visualization templates designed to convey complex data clearly and effectively within dynamic video contexts.
- **Algorithms.** We develop two algorithms to support robust visualization embedding in dynamic video scenes. The first estimates frame-by-frame camera poses, enabling visualizations to remain stably anchored to the background. The second computes and refines object trajectories across frames, allowing visualizations to accurately follow moving targets within the video.

2 RELATED WORK

In this section, we survey the papers that are most relevant to our work, including professional video editing software, embedded visualization, and point tracking.

2.1 Video Editing Software

Video editing is a broad field that involves various techniques, technologies, and tools used to create, manipulate, and refine video content, which often pose barriers to users [10], [11]. Professional video editing software offers powerful tools to insert animated objects into videos. Traditionally, users must manually keyframe an object's position, rotation, and scale over time, with smooth transitions achieved through interpolation. While recent advances have introduced automated tracking methods, such as 3D camera estimation and object tracking, these techniques, available in tools like Adobe After Effects, Blender, and Nuke [7], [8], [12], still require a level of expertise that can be challenging for beginners. At the same time, the growing demand for data-driven videos highlights a gap in current workflows: mainstream video editing tools lack integrated support for data visualization. Users often switch between separate tools or project files to create visualizations, making it difficult to assess whether a chart fits naturally within a given video context. Currently, no tool allows for direct editing of chart styles within the video environment while supporting real-time assessment, motion synchronization, and object tracking. This creates a pressing need for authoring tools that bridge the gap between visualization and video editing.

2.2 Embedded Visualization in Video

Embedded data visualization in videos has become increasingly popular [13]–[16]. However, this process often requires users to manually create keyframes for positioning the visualizations within the video. Recently, there has been increasing research on intelligent systems that can help embed visualizations in videos [6], [17]–[19]. Early works primarily focused on embedding static charts into videos. For instance, SmartShot [17] developed a system that optimizes the placement of charts to avoid obstructing the visual focus, ensuring aesthetic balance and readability. SwimFlow [18] explored how to embed visualizations into

swimming competition videos. Their system allows charts to animate by using manual annotations to mark athletes' starting positions and interpolating to calculate their motion trajectories. However, this approach is clearly limited when dealing with more complex motion patterns. Recent advancements in computer vision now enable the embedding of visualizations directly into sports videos, offering a more dynamic and adaptive solution. For instance, iBall [6] embeds dynamic visual data cues into basketball videos and automatically adjusts the information display based on the user's gaze. However, when the camera moves, the charts can only approximate the motion rather than being stably anchored to the scene. Additionally, these methods typically involve 2D overlays and tracking.

In contrast to these domain-specific solutions, our approach tracks 3D trajectories of arbitrary objects and supports 3D effects, including perspective transformations and occlusions of the inserted visualizations. Moreover, existing systems often lack the flexibility to freely create and edit visualizations to meet user-specific needs. In our system, users can directly edit the types, styles, and data mappings of charts on the video, streamlining the creation process and offering greater customization.

2.3 Point Tracking

Tracking arbitrary points in videos has witnessed substantial progress in recent years [20]–[22], with methods such as TAP-Net [23] demonstrating the ability to reliably follow both static and dynamic points throughout a video sequence. These approaches typically leverage appearance-based cues and temporal consistency to maintain accurate correspondences, even under significant motion and occlusion. However, focusing solely on 2D tracking is often insufficient in practical applications. While a dynamic point in the scene can be tracked frame-by-frame, certain use cases, such as visual overlays or interactive annotations, require this point to remain anchored relative to the static scene background, rather than to moving objects or transient visual cues. To achieve this, it becomes necessary to disentangle camera motion from scene dynamics, which calls for robust camera pose estimation.

Fortunately, a variety of mature techniques now exist for estimating camera pose from monocular or multi-view video streams [24], [25], ranging from classical SLAM-based pipelines [26]–[28] to deep learning methods [29]–[33]. The integration of 2D point tracking with camera pose estimation enables a more unified paradigm: tracking arbitrary points in 3D space. This formulation has recently attracted increasing attention [34]–[36], as researchers extend traditional 2D tracking frameworks into the 3D domain. For instance, SpatialTracker [36] is the first work specifically designed for the task of 3D point tracking. It estimates the 3D trajectory of arbitrary pixels by combining image features with monocular depth estimation, and propagates information through a graph neural network (GNN) to model long-range spatiotemporal motion. Similarly, TAPIR-3D [34] is an experimental extension of the original 2D point tracking model TAPIR, designed to output 3D point trajectories. It initializes keypoints in each frame, refines their 2D tracks using temporal context from adjacent frames, and

subsequently lifts them to 3D space using depth estimation models such as ZoeDepth [37].

We propose a novel approach that enhances the accuracy of 3D point tracking by integrating it with the practical requirements of embedding visualizations into real-world video content. Our system enables users to anchor visualizations to fixed locations within the scene or dynamically attach them to moving objects, regardless of camera motion or scene complexity. This flexibility allows for robust visualization embedding across a wide range of video scenarios.

3 SYSTEM DESIGN AND OVERVIEW

The *ChartBlender* system was motivated by our work experience on a data video design in collaboration with a prominent Chinese media organization. In this project, we were responsible for designing visualization charts and embedding the charts into a video. To support this task, we surveyed existing tools and systems for creating chart-embedded video. One notable system was VisTellar [9], which enables end-users to record short videos and embed data visualizations using augmented reality (AR) techniques. VisTellar tracks static elements in the video and anchors charts accordingly, offering a lightweight and mobile-friendly approach.

Although VisTellar is not open-source, we introduced it to our collaborators as a representative example of chart-embedded video tools. They noted, however, that end-users seldom embed charts into videos directly. In contrast, professional data journalists (our target users) require such capabilities but demand far greater precision and control. They highlighted three critical requirements: (1) accurate video motion tracking that can handle both static and dynamic objects; (2) compatibility with diverse video sources, including those lacking camera metadata, as is common in real-world media production; and (3) support for multiple dynamic charts within a single video, with fine-grained control over timing and placement to maintain contextual relevance and visual coherence.

We observed a significant gap in tools that enable seamless and efficient embedding of visualizations into real-world videos. In current practice, designers often resort to manually inserting pre-rendered charts frame by frame using software like Adobe After Effects. This process is so labor-intensive that a ten-second clip can require an entire day of work according to our own experience (see the example video¹ (2'44", 3'25") that we produced in this way). The majority of this effort goes into repetitive adjustments of position, scale, and orientation, rather than creative or analytical tasks. This inefficiency underscores the need for a dedicated authoring tool that can automate chart-video synchronization. Through close discussions with our collaborators, we distilled a set of core design requirements that guided the development of ChartBlender.

R1 Video-Suited Visualization Design. Visualizations should be designed to present data clearly while preserving the visual coherence of the scene, minimizing interference with the underlying video content.

R2 Depth-Aware Embedding. Visualizations should be embedded into the video by aligning with camera

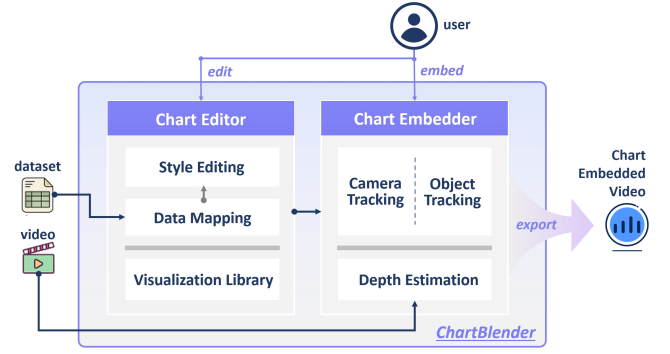


Fig. 1. *ChartBlender* system consists of two modules: Chart Editor and Chart Embedder.

depth and adopting a perspective consistent with the video scene. Such alignment ensures that the visualizations appear perceptually native to the scene, rather than as artificial post-production overlays.

R3 Motion Synchronization. As the video plays, the visualizations should move in synchrony with the video, including the movement of both the camera and objects in the scene. To achieve this synchronization, it is necessary to track camera and object motion accurately.

R4 Coordinated Multi-Chart Embedding. The system should support the integration of multiple visualizations within a single video, allowing authors to coordinate their spatial placement and temporal sequencing. This enables richer data storytelling and ensures that each chart appears at the appropriate moment and location in the visual narrative.

To fulfill these requirements, we developed the ChartBlender system. Fig. 1 illustrates the system architecture and the embedding pipeline. The system consists of two main modules: (1) the Chart Editor, and (2) the Chart Embedder. Generally, a user starts creating a visualization-embedded video by uploading a dataset and interactively configuring the visualization using the Chart Editor. This module allows users to customize various properties such as data mapping and style editing (R1). Afterward, users have a real-time preview of the chart's 3d placement and appearance within the video to the Chart Embedder (R2). The Chart Embedder incorporates a tracking algorithm that synchronizes visualizations with motion in the video and operates without requiring any camera metadata. It first performs depth estimation on the uploaded video, then anchors the visualization to the scene based on the user's selected tracking mode and target (R3). Finally, users can further adjust the chart, trim the timeline, and incorporate additional elements to produce smoother, more engaging, visualization-enhanced videos (R4). Collectively, these modules provide a lightweight yet powerful interactive workflow that automates chart embedding, reduces manual effort, and lowers the barrier for users. At the same time, the system supports the creation of visually coherent visualizations that integrate seamlessly into dynamic video scenes. While the Chart Editor functions as a relatively standard visualization creation module, in the following section, we focus on the Chart Embedder, which constitutes the core contribution of our system.

1. <http://edu.people.com.cn/n1/2023/0915/c1006-40078200.html>

4 CHART EMBEDDER

In this section, we present a tracking algorithm for synchronizing visualizations with video motion. The algorithm supports two scenarios: (1) keeping visualizations stably anchored to the background as the camera moves (*camera tracking*), and (2) allowing visualizations to follow moving objects within the scene (*object tracking*).

As shown in Fig. 2, given an input video consisting of N frames and a user-specified target point (x, y) , our goal is to generate a sequence of 3D pose matrices O_t . Each pose matrix represents the position and rotation of the tracked point in 3D space at frame t . It begins with *depth estimation* (Fig. 2 (a)) from the input video frames, which produces per-frame depth maps. These maps are used in two parallel modules: *camera tracking* (Fig. 2 (b)), which computes frame-to-frame transformations and accumulates them into a global camera pose; and *object tracking* (Fig. 2 (c)), which tracks a user-specified point across frames and combines its 2D trajectory with depth information to estimate a smoothed 3D object pose. Finally, the estimated object pose is applied to the visualization, which is then overlaid onto the video scene.

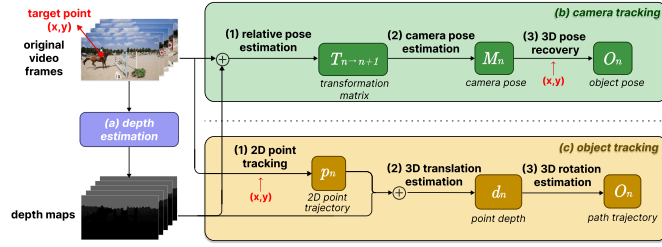


Fig. 2. The pipeline of the Chart Embedder.

4.1 Depth Estimation

Our system employs a monocular depth estimation model, *Metric3D* [38], to generate per-frame metric depth maps directly from original video frames. The major advantages of adopting *Metric3D* are twofold: (1) it predicts absolute metric depth without requiring ground-truth depth or camera intrinsics, enabling zero-shot deployment on in-the-wild videos; (2) it achieves high generalization capability across scenes, owing to its large-scale training on diverse data.

Given these benefits, we apply *Metric3D* to each of the N video frames to generate a sequence of dense depth maps D_n , $n \in 0, 1, \dots, N-1$. For a user-specified 2D point (x, y) , we can extract its first frame's depth value from the depth map as $d = D_0(x, y)$. This depth information serves as a crucial foundation for the subsequent camera tracking and object tracking processes, enabling accurate spatial reasoning in both modules.

4.2 Camera Tracking

In ChartBlender, camera tracking ensures that embedded 3D visualizations remain spatially consistent with the static element throughout the video (Fig. 3(a)). To achieve this, we estimate the camera's motion through a three-step process. First, we perform (1) **relative pose estimation** to compute the geometric transformation between adjacent video

frames, capturing how the camera moves over time. This information is then used in (2) **camera pose estimation**, accumulating relative transformations to recover the camera's trajectory in the scene. Finally, we conduct (3) **3D pose recovery** to infer the camera's position and orientation in 3D space, enabling visualizations to be accurately projected.

Relative pose estimation. To understand how the camera moves from frame to frame, we should estimate the relative transformation between each pair of consecutive video frames. These pairwise transformations form the foundation for reconstructing the full camera trajectory. We employ an RGBD odometry model provided by Open3D [39], [40] to compute the relative camera motion between adjacent RGBD frames. Given two consecutive frames n and $n+1$, RGBD odometry estimates a transformation matrix. Specifically, we extract a transformation matrix $T_{n \rightarrow n+1}$ that aligns the RGB and depth images. Each transformation is a 4×4 homogeneous transformation matrix composed of a rotation matrix $R_{n \rightarrow n+1}$ and a translation vector $t_{n \rightarrow n+1}$:

$$T_{n \rightarrow n+1} = \begin{bmatrix} R_{n \rightarrow n+1} & t_{n \rightarrow n+1} \\ 0 & 1 \end{bmatrix} \quad (1)$$

Camera pose estimation. While relative poses describe local motion between frames, embedding visualizations in a stable, world-aligned coordinate system requires each frame's absolute camera pose. This enables consistent rendering of the 3D object across the video sequence. We compute the absolute camera pose M_n at each frame n by chaining all previous relative transformations starting from the first frame:

$$M_n = T_{1 \rightarrow 2} T_{2 \rightarrow 3} \dots T_{n-1 \rightarrow n} \quad (2)$$

This accumulation step reconstructs the global camera trajectory, allowing us to express each frame's viewpoint in the same coordinate system.

3D pose recovery. To render the 3D visualization as if it were physically anchored in the scene, we must compute its position in the global world coordinate system. Given a user-specified 2D point (x, y) in the image and its corresponding predicted depth d , we first back-project the point into the **3D camera coordinate system** using the inverse of the camera intrinsic matrix K^{-1} . The resulting 3D point in the camera frame is:

$$P_n = K^{-1} \cdot (d_0 \cdot \tilde{o}_n) \quad (3)$$

where P_n denotes the 3D position of a tracked point at frame n , $\tilde{o}_n = [x, y, 1]^T$ is the homogeneous pixel coordinate. Next, we transform this point into the **world coordinate system** using the inverse of the absolute camera pose M_n , computed from accumulated relative poses. The object's global pose O_n is then given by:

$$O_n = M_n^{-1} \cdot P_n \quad (4)$$

This transformation places the 3D visualization at a consistent location in the world coordinate system, regardless of camera motion. It ensures that the visualization remains spatially stable and visually aligned with the static background in the video.



Fig. 3. An illustration of the two motion embedding modes supported by our system: *Camera Tracking* and *Object Tracking*. In the *Camera Tracking* mode, the visualization remains anchored to a fixed point in the scene, attaching a chart to a stationary fence in the video. In contrast, *Object Tracking* binds the visualization to a moving object, attaching a chart to a galloping horse.

4.3 Object Tracking

In ChartBlender, the goal of object tracking is to enable visualizations to remain spatially aligned with moving elements in the video scene (Fig. 3(b)). To achieve this, we estimate the 3D motion of target objects from monocular video input through a three-stage pipeline. First, we perform **(1) 2D point tracking** to extract the object’s pixel-wise trajectory across frames, capturing how it moves within the image plane. This trajectory serves as the basis for the second stage, **(2) 3D translation estimation**, which lifts the 2D motion into 3D space to approximate the object’s position relative to the camera over time, allowing visualizations to maintain consistent placement as the object moves. Finally, we perform **(3) 3D rotation estimation** to recover the object’s orientation changes, ensuring that embedded visualizations can rotate coherently with the object’s local motion, further enhancing the perceptual integration.

2D point tracking. We begin by identifying salient points on dynamic objects and tracking their 2D positions across frames. To accomplish this, we use BootsTAP [41], a high-precision keypoint tracking algorithm that leverages dense visual correspondence estimation. For each target point (x, y) , the tracker generates a pixel-level trajectory over time, denoted as $p_n = (u_n, v_n) \rightarrow p_{n+1} = (u_{n+1}, v_{n+1})$. The 2D trajectories capture the apparent motion of object features in image space and form the foundation for estimating real-world displacement in 3D, which is critical for subsequent motion reconstruction.

3D translation estimation. To reconstruct the spatial motion of tracked points, we lift the 2D trajectories to 3D space. For each frame, the 2D trajectory is projected into 3D space using the depth map of the tracked point in the camera coordinate system.

$$d_n = D_n(p_n) \quad (5)$$

However, monocular depth estimates are inherently noisy and temporally unstable due to factors such as low-texture regions, occlusions, and variations in lighting. These inconsistencies can lead to jitter and discontinuities in the reconstructed 3D trajectories, especially when tracking fine-grained object motion. Such artifacts degrade both the physical plausibility and visual coherence of the motion path, undermining downstream tasks like 3D alignment and visualization anchoring. To address this, we apply temporal

smoothing to the depth signal using quadratic regression over a sliding window:

$$\hat{d}_n = \text{QuadraticRegression}(d_n) \quad (6)$$

As previously defined in Equation (3), we recover the 3D translation vector t_n of the target point in the camera coordinate system by back-projecting its 2D image coordinate using the estimated depth and the intrinsic matrix K .

3D rotation estimation. Finally, we estimate object rotation based on the direction of motion in 3D space to ensure that visualizations remain properly oriented when attached to moving objects. Specifically, we define the per-frame motion vector as $V_n = P_{n+1} - P_n$. We obtain the rotation vector R_n by constraining the object’s local X axis to follow V_n . To support stable rotation estimation, we first regularize the raw 3D point trajectories by minimizing sudden changes in displacement. This is implemented as a second-order temporal smoothing loss:

$$\min_{\hat{P}} \sum_n \|\hat{P}_{n+1} - \hat{P}_n\|^2 + \lambda \sum_n \|\hat{P}_{n+2} - 2\hat{P}_{n+1} + \hat{P}_n\|^2 \quad (7)$$

Next, we apply the same principle in the velocity domain to ensure that the direction of motion also varies smoothly over time. The corresponding velocity regularization is formulated as:

$$\mathcal{L}(V_n) = \sum_n \|V_{n+1} - V_n\|^2 + \lambda \sum_t \|V_{n+1} - 2V_n + V_{n-1}\|^2 \quad (8)$$

This second-order smoothing constraint encourages both consistent motion direction and smooth acceleration profiles, mitigating jitter and improving temporal coherence in the estimated trajectories. Given the smoothed translation vector and rotation vector, the final object pose at each frame is defined as $O_n = \{R_n \mid t_n\}$.

5 CHARTBLENDER

In this section, we introduce the interface design, visualization design, and interaction.

5.1 User Interface

The user interface, as shown in Fig. 4, consists of three major views: **the Chart View** (Fig. 4-1), **the Video View** (Fig. 4-2), and **the Timeline View** (Fig. 4-3). In the Chart View, users can upload a dataset, after which the raw data is displayed directly within the view. Users can then choose a chart

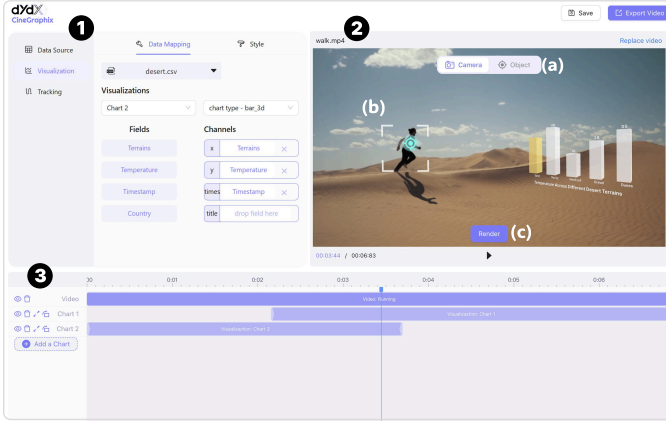


Fig. 4. The interface consists of three main components: (1) the Chart View for creating and editing visualizations, (2) the Video View for embedding charts and previewing the embedding result, and (3) the Timeline View for adding, removing, and trimming chart segments.

type (e.g., **bar chart**, **line chart**, **area chart**, and **text**) and define encoding mappings by dragging data fields to visual channels such as the **x-axis**, **y-axis**, **timestamp**, or **title**. To refine the visual presentation, users can adjust stylistic properties including line thickness, color, and theme (R1). The Video View provides a real-time preview of the current video frame. Users can manipulate the visualization’s position, rotation, and scale in 3D space, enabling precise spatial embedding within the scenes (R2). To synchronize visualizations with video motion, users first select a motion mode, either **camera tracking** or **object tracking** (Fig.4-2(a)), and then specify target points in the video as tracking anchors (Fig.4-2(b)). After configuration, clicking the **Render** button (Fig.4-2(c)) triggers the system to compute the visualization’s motion path and composite it into the video (R3). Once rendering is complete, users can click the **Play** button to preview the embedded visualization in motion, ensuring alignment and visual consistency.

The Timeline View serves as an editing panel that supports temporal coordination and layer management. On the left side of the interface, users can add, delete, or lock chart layers to organize content across multiple visualization tracks. On the right side, a **Timeline** allows users to control the duration and timing of each chart via intuitive drag, stretch, and trim interactions (R4). Finally, by clicking the **Export** button, users can generate the composite video with the embedded visualizations synchronized to the video.

5.2 Visualization Design

Our goal is to design visualizations that are well-suited for integration within videos. This requires rethinking how charts are structured and styled to maintain both visual clarity and contextual harmony in videos [42]. To this end, we collected a total of 200 high-quality videos and manually segmented them into 502 clips, each containing at least one embedded visualization. As shown in Fig. 6, these videos span ten diverse domains. We also analyzed the most commonly used chart types across the dataset. Furthermore, we identified several recurring design patterns in how visualizations are embedded within real-world video content. These patterns are summarized as follows.

First, a majority of charts (130 cases) incorporate background to improve readability, with a subset (21) employing semi-transparent backgrounds to maintain visual access to the underlying scene. Notably, gridlines were selectively applied to support data interpretation, with horizontal guides appearing more frequently (109) than vertical ones (43), while 64 charts omitted them entirely. Second, very few charts (only 4) included legends, indicating a general preference for minimalist presentations in time-constrained video contexts. Nevertheless, essential structural components such as axes (retained in 171 charts) and titles (present in 168 charts) were commonly preserved. Third, when visualizations were associated with specific objects in the scene, designers frequently employed visual linking strategies to establish a clear connection between the chart and its target (68). These strategies included directional cues such as arrows, lines, and bounding boxes. The choice of pointer type often varied depending on scene complexity: in simple scenes with few moving objects, minimal indicators such as triangles were typically sufficient; in more complex scenes with multiple overlapping motions, designers commonly used bounding boxes or anchored pointers to more clearly distinguish the tracked target.

These findings highlight a set of implicit yet widely adopted design patterns for video-suited visualizations design, which we synthesize into a structured design space, as illustrated in Fig. 5. This design space is organized along two key dimensions: the motion mode and the visualization type. It distinguishes between two modes of motion (object tracking and camera tracking) corresponding to whether the visualization follows a moving target in the scene or remains fixed relative to the global environment. Horizontally, it categorizes common visualization types, including text annotations, line charts, area charts, bar charts, and 3D charts, as well as their corresponding linking and layout strategies (e.g., aiming lines, bounding boxes, or indicators). Based on this design space, we developed a visualization chart library using Three.js, providing a collection of chart templates optimized for embedding in dynamic video scenes.

5.3 Interaction

To support efficient visualization authoring and seamless synchronization within video, we propose a set of interactions in ChartBlender:

Upload. Users can upload datasets and video files either by clicking the upload button or by dragging and dropping files into the designated panel.

Data Mapping. Data attributes can be mapped to visual channels through direct manipulation: users drag data fields onto chart elements to define encoding relationships.

Zoom and Pan. Users can interactively adjust the visualization view: left-click and drag to reposition charts, scroll to zoom in and out, and right-click and drag to rotate.

Chart and Style Switching. Users can switch between different chart types via tabs in the interface. They can also adjust visual styling, such as color schemes, by clicking style options or using a color picker tool.

Anchor Selection. To ensure accurate chart placement, users can click on static or dynamic objects in the video to define visual anchor points. These anchors are used to bind

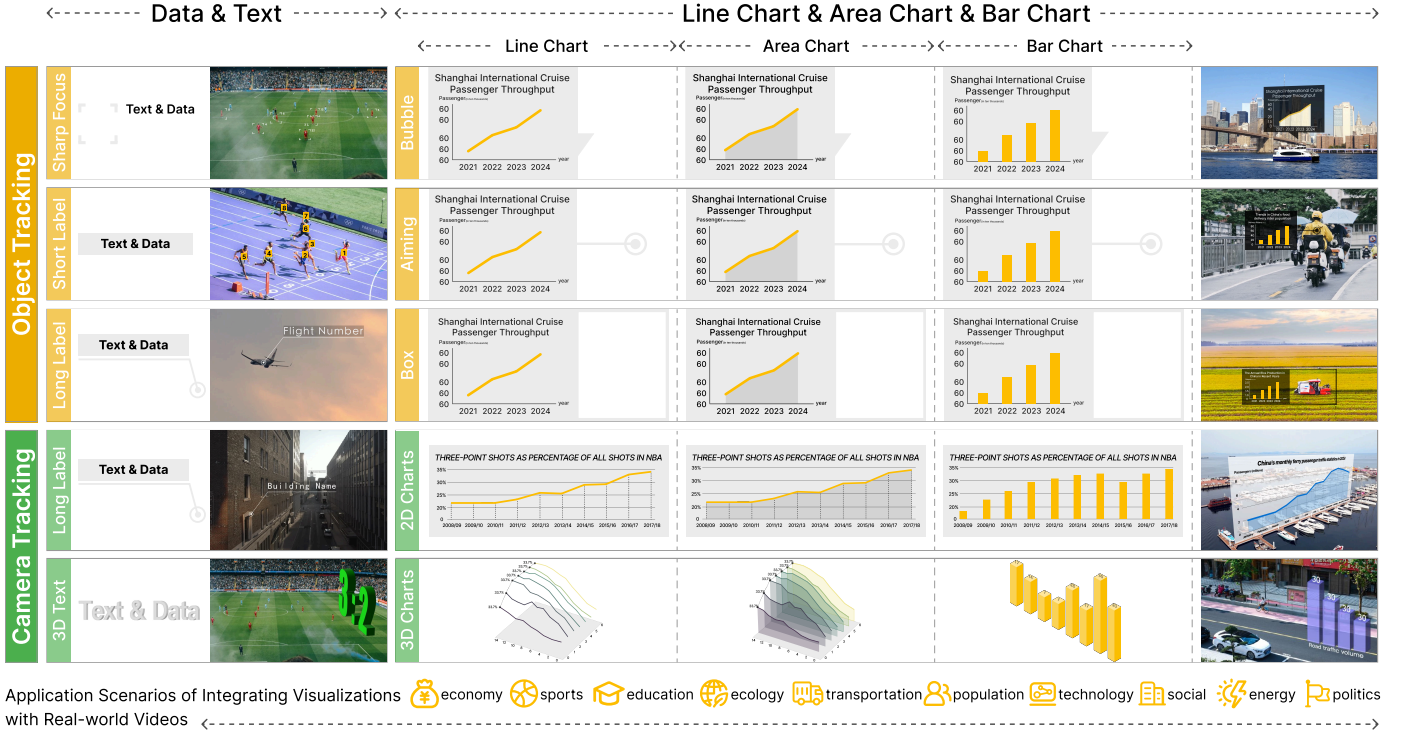


Fig. 5. Design space for visualizations suitable for embedding in video, which illustrates five representative visualization forms combined with two motion anchoring strategies (object tracking and camera tracking). It reveals common design patterns for how visualizations are structured and integrated within dynamic video scenes across diverse real-world applications.

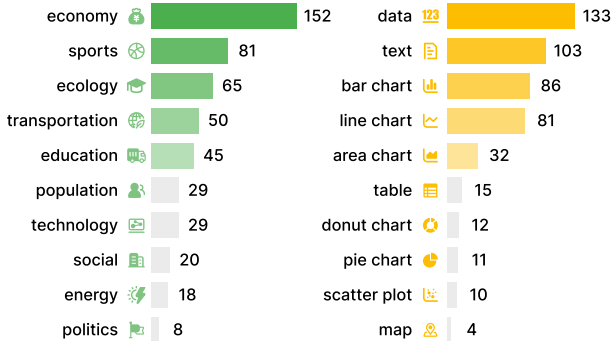


Fig. 6. Distribution of chart types and video domains.

visualizations to specific elements in the scene, supporting consistent spatial alignment across frames.

Track Editing. Users can manage chart tracks via the timeline view. Tracks can be added or removed by clicking the corresponding buttons in the toolbar on the left. On the right, users can adjust the timing and duration of each chart by dragging chart tracks directly along the timeline.

6 EVALUATION

We evaluated the *ChartBlender* and the key techniques through three approaches: (1) a quantitative experiment to assess the precision of camera tracking, (2) a quantitative experiment to assess the precision of object tracking, and (3) domain expert interviews to evaluate the overall usability of the system.

6.1 Camera Tracking Precision

In our system, camera tracking is implemented using RGBD odometry, which estimates frame-by-frame camera motion by leveraging both RGB appearance and depth information. As a result, the quality of depth estimation plays a critical role in the precision of camera tracking. To evaluate this dependency, we compare how different monocular depth models affect the overall pose estimation performance of the RGBD odometry pipeline.

Experimental Setup. To evaluate the impact of depth estimation quality on camera pose recovery, we conducted a comparative experiment using different monocular depth models combined with RGBD odometry. Specifically, we compared *Metric3D*, which emphasizes metric depth precision, with *ZoeDepth*, which focuses on generalization and temporal consistency. We refer to the two pipelines as *Metric3D + RGBD odometry* (our proposed method) and *ZoeDepth + RGBD odometry* (baseline). We selected a subset of the *DriveTrack* dataset [43], consisting of 18 video sequences (1,806 frames in total), where camera motion was sufficiently pronounced and affected by dynamic foreground objects. For each method, predicted depth maps were fed into RGBD odometry implemented in *Open3D* [39], which uses a hybrid geometric-photometric optimization [40] to estimate per-frame camera extrinsics. A fixed intrinsic matrix of the form [1000, 1000, width/2, height/2] was used for all sequences.

Evaluation Metric. To quantitatively evaluate the precision of our camera tracking approach and assess the influence of different depth estimation models, we measured the geometric discrepancy between the estimated camera poses

and the ground-truth extrinsics provided by the TAPVid-3D dataset [34]. For each frame, we compared the predicted camera pose ($R_{\text{pred}}, t_{\text{pred}}$) with the corresponding ground-truth pose ($R_{\text{gt}}, t_{\text{gt}}$), and computed both rotation and translation errors. The rotation error was defined as the angular difference between the predicted and ground-truth orientations. Specifically, we first computed the relative rotation matrix $\Delta R = R_{\text{gt}}^{-1} R_{\text{pred}}$, and then calculated the rotation error as the angle of this rotation:

$$\theta = \arccos \left(\frac{\text{trace}(\Delta R) - 1}{2} \right), \quad (9)$$

This formulation captures the minimum angular difference between the two rotation matrices in 3D space. The translation error was defined as the Euclidean distance between the predicted and ground-truth camera positions:

$$\text{translation_error} = \|t_{\text{gt}} - t_{\text{pred}}\|. \quad (10)$$

Together, these two metrics quantify both orientation and positional discrepancies in the estimated camera trajectories. To evaluate overall precision and robustness to outliers, we report both the mean and median rotation and translation errors computed across all frames in the dataset.

Results and Analysis. As shown in Table 1, *Metric3D* consistently outperformed *ZoeDepth* in both rotation and translation precision when paired with RGBD odometry, achieving lower mean and median errors across all frames. Although both methods operate under the same fixed intrinsic setting, *Metric3D* provided more reliable metric depth, enabling more accurate frame-by-frame camera pose estimation. Another key reason for adopting *Metric3D* is its robustness in unconstrained environments where intrinsic calibration is unavailable, a common challenge in user-generated or in-the-wild videos. Despite the use of an approximate intrinsic matrix, the *Metric3D* + RGBD odometry pipeline maintained strong performance.

TABLE 1
Comparison on camera tracking. (Camera pose estimation errors)

Method	Rotation Error (degrees)		Translation Error (m)	
	Mean ↓	Median ↓	Mean ↓	Median ↓
Metric3D + RGBD odometry (ours)	8.641	8.851	6.518	6.432
ZoeDepth + RGBD odometry	10.544	11.061	7.598	7.610

6.2 Object Tracking Precision

We evaluated our system’s object tracking techniques by assessing the precision of the reconstructed 3D motion trajectories for dynamic objects. This reflects how well the system can estimate object movement in physical space.

Experimental Setup. In our system, object tracking is implemented by combining 2D keypoint tracking with monocular depth estimation to recover the 3D trajectories of dynamic objects across time. This process is essential for enabling visualization alignment with moving targets in the scene. The overall tracking precision depends on the quality of both the 2D keypoint trajectories and the estimated depth maps used for lifting to 3D. To evaluate this component, we conducted a systematic comparison of different tracking configurations by varying the underlying 2D tracking and

depth estimation models. Specifically, we considered two keypoint tracking models, *TAPIR* [44] and *BootsTAPIR* [41], and two depth estimation models, *ZoeDepth* and *Metric3D*, resulting in **four** combinations in total.

We performed this evaluation on a subset of the *PStudio* dataset [45], consisting of 36 video sequences (10,800 frames in total). These sequences feature clearly observable dynamic objects with prominent motion and minimal camera movement, allowing us to isolate object trajectory estimation from background motion. For each combination, 2D keypoints were first tracked across frames using the selected tracking model. These trajectories were then lifted into 3D space by back-projecting the 2D points with the corresponding depth estimates.

Evaluation Metric. We adopted the *Average 3D Point Distance* (APD_{3D}) metric, introduced in TAPVid-3D [34], to evaluate the precision of 3D point tracking. This metric quantifies the proportion of predicted 3D points that lie within a specified Euclidean distance threshold of their corresponding ground-truth positions, averaged over time and across tracked points. A higher value reflects better spatial precision and temporal consistency of the reconstructed trajectories.

Formally, the metric is defined as:

$$\text{APD}_{3D} \equiv \frac{1}{V} \sum_{i,t} v_t^i \cdot \mathbf{1} \left(\|\hat{P}_t^i - P_t^i\| < \delta_{3D}(P_t^i) \right), \quad (11)$$

where \hat{P}_t^i and P_t^i denote the predicted and ground-truth 3D positions of the i -th point at time t , v_t^i is a visibility indicator, and V is the total number of visible points. To quantify performance across different levels of precision, we report APD_{3D} under a fixed set of distance thresholds: [0.04, 0.08, 0.16, 0.32, 0.64].

Results and Analysis. As shown in TABLE 2, *BootsTAPIR* consistently outperformed *TAPIR* across all configurations, confirming its superior capability in 2D temporal keypoint tracking. With regard to depth estimation, our primary objective is not to reconstruct metrically accurate 3D geometry, but to generate perspective-consistent visualizations that preserve spatial coherence between foreground and background elements. In this context, moderate depth errors are acceptable, provided that the overall depth structure remains stable and visually plausible.

TABLE 2
Comparison on object tracking. (Average 3D point distance (APD_{3D})).

Method	APD _{3D} (↑)
BootsTAPIR + Metric3D (ours)	0.3424
TAPIR + Metric3D	0.3416
BootsTAPIR + ZoeDepth	0.3609
TAPIR + ZoeDepth	0.3595

6.3 Expert Interview

To further evaluate the usability of *ChartBlender*, a series of interviews with five data journalists (denoted as E1-E5) were performed. They had over 5 years’ video editing experiences on average, and were very familiar with chart-embedded videos. All participants provided informed consent prior to the study.

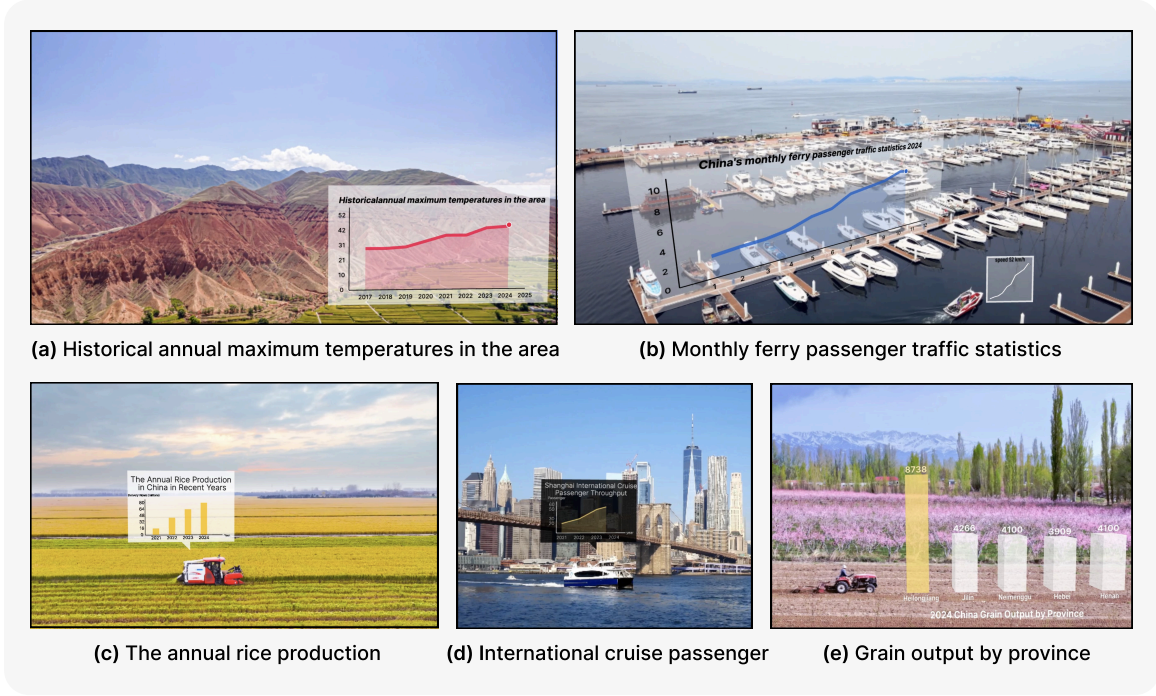


Fig. 7. Five example videos with embedded visualizations generated using *ChartBlender*

Procedure. The interviews were performed via an online meeting system. Each interview started by a 10-minute introduction about the system. Participants were first introduced to our system through a brief tutorial delivered by authors, and were given two task:

Task 1 - Goal-oriented (10 minutes). Participants are shown an example video that they have to reproduce. The result should consist of a bar chart that remains fixed in the field and an area chart that moves along with the vehicle.

Task 2 - Open-ended (30 minutes). Participants are asked to create two novel data videos by choosing among 10 short video clips (10" duration on average).

Finally, the experts were asked to finish a questionnaire, followed by an interview after they explored the functionalities of *ChartBlender*. The whole process lasted for about one hour, and the interviews were recorded for analysis.

Result. Fig. 7 presents sample videos generated by expert users using our system. In follow-up interviews, the experts offered a range of insightful comments, which are summarized as follows:

Fast Crafting. All experts agreed that our system was highly effective in supporting both camera tracking and object tracking. In particular, E1 commented that "This system can accomplish the work of several hours, or even days, in just two or three minutes." E2 mentioned that "This system allows me to see the real-time effect of chart edits in the video... I no longer need to repeatedly switch between project files, which used to waste a lot of time." E5 also noted that "The speed of result generation is so fast that I can quickly create multiple demos to observe where the chart embedding works best in the video."

Accurate Results. Most experts were very satisfied with our results, both for camera and object tracking (E1, E2, E4, E5). E1 commented, "The results are directly usable." E2 suggested that "The object tracking technique amazed me; it

not only takes the camera pose into account but also integrates the movement of the objects." E5 mentioned, "This result is more accurate than manual alignment."

A Professional and Elegant System. All the experts were satisfied with the system. Additionally, all of them mentioned that the system was very user-friendly and that they would recommend it to others. Specifically, they appreciated how seamlessly the system integrates chart creation and embedding into videos, accomplishing highly professional tasks (E1, 2, 5). E1 mentioned that "This system can complete highly professional tasks without requiring extensive skills or knowledge." E5 noted that "the chart can be translated and rotated in 3D, and it integrates seamlessly with the video." They were also satisfied with the chart creation aspect. E4 noted that "the data mapping feature eliminated the need for selecting data and creating visualizations in 3D software." E5 commented that "The chart creation process is very user-friendly for me. There are many expressive templates available for me to use ... Previously, I had to spend a lot of time on creating visualizations."

7 LIMITATIONS AND FUTURE WORK

Despite the encouraging evaluation results, several discussions and limitations were identified during the design and implementation process or mentioned by the experts during interviews. We hope to guide potential future research directions by pointing out these limitations.

Context-Aware Visualization Generation. Several experts (E1, E2, E4) expressed the need for a more intelligent system capable of understanding both dataset and video semantics. For instance, the system could automatically suggest visualization color schemes aligned with the video or incorporate domain-specific visual metaphors, such as rendering bars in a bar chart as crops in agricultural contexts. It could also

generate appropriate chart titles based on the video narrative and the underlying data. Future work may explore fine-tuning large language models (LLMs) to support automatic topic analysis, enabling the system to generate context-aware visualizations with optimized design elements, enhancing the coherence and quality of data-driven videos.

Layered Rendering. Although the current system supports depth-aware relationships between charts, Several experts (E1, E3) highlighted the potential of masking functionality that enables visualizations to be occluded by foreground objects in the video. Such a feature would allow charts to appear partially or fully behind scene elements, enhancing realism and spatial coherence.

Tracking Editing. Currently, the system automatically generates motion trajectories for embedded charts based on anchor points. A promising extension is to introduce a visual trajectory editor that renders the underlying coordinate array as editable curves within a canvas or SVG-based interface. Leveraging techniques such as spline interpolation, draggable control points, and direct path manipulation, users could intuitively modify the motion path. Such an interface would offer frame-level control over trajectory shapes, allowing insertion, deletion, and adjustment of key-points. This would significantly enhance the flexibility and expressiveness of the authoring workflow.

8 CONCLUSION

In this paper, we introduced *ChartBlender*, an integrated system for authoring, embedding, and synchronizing data visualizations within dynamic video content. By combining computer vision algorithms for camera and object tracking, we enable synchronization between visualizations and video motion. In addition, the system incorporates an interactive workflow to support easy and efficient authoring of videos with visualizations embedded. Quantitative evaluations demonstrate the effectiveness of our tracking algorithms in recovering spatially consistent motion trajectories. Additionally, interviews with domain experts confirm the system's usability, expressiveness, and potential for professional media production. The evaluation showed the power of *ChartBlender* system and revealed several limitations of the current system, which will be addressed in the future.

ACKNOWLEDGMENTS

Nan Cao is the corresponding author. This work was supported by the National Key Research and Development Program of China (2023YFB3107100). We would like to thank all the reviewers for their valuable feedback.

REFERENCES

- [1] Q. Chen, S. Cao, J. Wang, and N. Cao, "How does automation shape the process of narrative visualization: A survey of tools," *IEEE TVCG*, vol. 30, no. 8, pp. 4429–4448, 2024.
- [2] F. Amini, N. Henry Riche, B. Lee, C. Hurter, and P. Irani, "Understanding data videos: Looking at narrative visualization through the cinematography lens," in *Proceedings of the 33rd Annual ACM conference on human factors in computing systems*, 2015, pp. 1459–1468.
- [3] D. Shi, F. Sun, X. Xu, X. Lan, D. Gotz, and N. Cao, "Autoclips: An automatic approach to video generation from data facts," in *Computer Graphics Forum*, vol. 40, no. 3. Wiley Online Library, 2021, pp. 495–505.
- [4] Y. He, K. Xu, S. Cao, Y. Shi, Q. Chen, and N. Cao, "Leveraging foundation models for crafting narrative visualization: A survey," *IEEE TVCG*, pp. 1–20, 2025.
- [5] W. Willett, Y. Jansen, and P. Dragicevic, "Embedded data representations," *IEEE TVCG*, vol. 23, no. 1, pp. 461–470, 2017.
- [6] C. Zhu-Tian, Q. Yang, J. Shan, T. Lin, J. Beyer, H. Xia, and H. Pfister, "iball: Augmenting basketball videos with gaze-moderated embedded visualizations," in *Proceedings of the 2023 CHI Conference on Human Factors in Computing Systems*, ser. CHI '23. New York, NY, USA: Association for Computing Machinery, 2023. [Online]. Available: <https://doi.org/10.1145/3544548.3581266>
- [7] "Adobe After Effects," 2022. [Online]. Available: <https://www.adobe.com/products/aftereffects.html>
- [8] "Blender," 2023. [Online]. Available: <https://www.blender.org>
- [9] W. Tong, K. Shigyo, L.-P. Yuan, M. Fan, T.-C. Pong, H. Qu, and M. Xia, "Vistellar: Embedding data visualization to short-form videos using mobile augmented reality," *IEEE TVCG*, vol. 31, no. 3, pp. 1862–1874, 2025.
- [10] B. Wang, Y. Li, Z. Lv, H. Xia, Y. Xu, and R. Sodhi, "Lave: Llm-powered agent assistance and language augmentation for video editing," in *Proceedings of the 29th International Conference on Intelligent User Interfaces*, ser. IUI '24. New York, NY, USA: Association for Computing Machinery, 2024, p. 699–714. [Online]. Available: <https://doi.org/10.1145/3640543.3645143>
- [11] H. Duan, J. Liao, L. Lin, A. El Saddik, and W. Cai, "Meeter: A human-centered automatic video editing system for meeting recordings," *ACM Trans. Multimedia Comput. Commun. Appl.*, vol. 20, no. 9, Aug. 2024. [Online]. Available: <https://doi.org/10.1145/3648681>
- [12] "Nuke," 2022. [Online]. Available: <https://www.foundry.com/>
- [13] F. Amini, N. H. Riche, B. Lee, A. Monroy-Hernandez, and P. Irani, "Authoring data-driven videos with dataclips," *IEEE TVCG*, vol. 23, no. 1, pp. 501–510, 2017.
- [14] Y. Shi, X. Lan, J. Li, Z. Li, and N. Cao, "Communicating with motion: A design space for animated visual narratives in data videos," in *Proceedings of the 2021 CHI Conference on Human Factors in Computing Systems*, ser. CHI '21. New York, NY, USA: Association for Computing Machinery, 2021. [Online]. Available: <https://doi.org/10.1145/3411764.3445337>
- [15] X. Lan, X. Xu, and N. Cao, "Understanding narrative linearity for telling expressive time-oriented stories," in *Proceedings of the 2021 CHI Conference on Human Factors in Computing Systems*, ser. CHI '21. New York, NY, USA: Association for Computing Machinery, 2021. [Online]. Available: <https://doi.org/10.1145/3411764.3445344>
- [16] L. Yang, X. Xu, X. Lan, Z. Liu, S. Guo, Y. Shi, H. Qu, and N. Cao, "A design space for applying the freytag's pyramid structure to data stories," *IEEE TVCG*, vol. 28, no. 1, p. 922–932, Jan. 2022. [Online]. Available: <https://doi.org/10.1109/TVCG.2021.3114774>
- [17] T. Tang, J. Tang, J. Lai, L. Ying, Y. Wu, L. Yu, and P. Ren, "Smartshots: An optimization approach for generating videos with data visualizations embedded," *ACM TIS*, vol. 12, no. 1, Mar. 2022. [Online]. Available: <https://doi.org/10.1145/3484506>
- [18] L. Yao, R. Vuillemot, A. Bezerianos, and P. Isenberg, "Designing for visualization in motion: Embedding visualizations in swimming videos," *IEEE TVCG*, vol. 30, no. 3, pp. 1821–1836, 2024.
- [19] C. Zhu-Tian, S. Ye, X. Chu, H. Xia, H. Zhang, H. Qu, and Y. Wu, "Augmenting sports videos with viscommentator," *IEEE TVCG*, vol. 28, no. 1, p. 824–834, Jan. 2022. [Online]. Available: <https://doi.org/10.1109/TVCG.2021.3114806>
- [20] X. Zhou, V. Koltun, and P. Krähenbühl, "Tracking objects as points," in *ECCV*. Springer, 2020, pp. 474–490.
- [21] S. Gauglitz, T. Höllerer, and M. Turk, "Evaluation of interest point detectors and feature descriptors for visual tracking," *International journal of computer vision*, vol. 94, pp. 335–360, 2011.
- [22] X. Zhou, V. Koltun, and P. Krähenbühl, "Tracking objects as points," in *Computer Vision – ECCV 2020*, A. Vedaldi, H. Bischof, T. Brox, and J.-M. Frahm, Eds. Cham: Springer International Publishing, 2020, pp. 474–490.
- [23] R. Hu, J. Xu, B. Chen, M. Gong, H. Zhang, and H. Huang, "Tap-net: transport-and-pack using reinforcement learning," *ACM TOG*, vol. 39, no. 6, pp. 1–15, 2020.
- [24] M. Xu, Y. Wang, B. Xu, J. Zhang, J. Ren, Z. Huang, S. Poslad, and P. Xu, "A critical analysis of image-based camera pose estimation techniques," *Neurocomputing*, vol. 570, p. 127125, 2024.

- [25] J. Guan, Y. Hao, Q. Wu, S. Li, and Y. Fang, "A survey of 6dof object pose estimation methods for different application scenarios," *Sensors*, vol. 24, no. 4, p. 1076, 2024.
- [26] C. Campos, R. Elvira, J. J. G. Rodríguez, J. M. Montiel, and J. D. Tardós, "Orb-slam3: An accurate open-source library for visual, visual-inertial, and multimap slam," *IEEE transactions on robotics*, vol. 37, no. 6, pp. 1874–1890, 2021.
- [27] A. R. Vidal, H. Rebecq, T. Horstschaefer, and D. Scaramuzza, "Ultimate slam? combining events, images, and imu for robust visual slam in hdr and high-speed scenarios," *IEEE Robotics and Automation Letters*, vol. 3, no. 2, pp. 994–1001, 2018.
- [28] R. Mur-Artal, J. M. M. Montiel, and J. D. Tardós, "Orb-slam: A versatile and accurate monocular slam system," *IEEE Transactions on Robotics*, vol. 31, no. 5, pp. 1147–1163, 2015.
- [29] Y. Shavit and R. Ferens, "Introduction to camera pose estimation with deep learning," *arXiv preprint arXiv:1907.05272*, 2019.
- [30] J. L. Schonberger and J.-M. Frahm, "Structure-from-motion revisited," in *CVPR*, 2016, pp. 4104–4113.
- [31] J. Hidalgo-Carrió, G. Gallego, and D. Scaramuzza, "Event-aided direct sparse odometry," in *CVPR*, June 2022, pp. 5781–5790.
- [32] T. Zhou, M. Brown, N. Snavely, and D. G. Lowe, "Unsupervised learning of depth and ego-motion from video," in *CVPR*, 2017, pp. 1851–1858.
- [33] S. En, A. Lechervy, and F. Jurie, "Rpnet: An end-to-end network for relative camera pose estimation," in *ECCV*, 2018, pp. 0–0.
- [34] S. Koppula, I. Rocco, Y. Yang, J. Heyward, J. Carreira, A. Zisserman, G. Brostow, and C. Doersch, "Tapvid-3d: A benchmark for tracking any point in 3d," *arXiv preprint arXiv:2407.05921*, 2024.
- [35] E. Yu, K. Blackburn-Matzen, C. Nguyen, O. Wang, R. Habib Kazi, and A. Bousseau, "Videodoodles: Hand-drawn animations on videos with scene-aware canvases," *ACM TOG*, vol. 42, no. 4, pp. 1–12, 2023.
- [36] Y. Xiao, Q. Wang, S. Zhang, N. Xue, S. Peng, Y. Shen, and X. Zhou, "Spatialtracker: Tracking any 2d pixels in 3d space," in *CVPR*, 2024, pp. 20 406–20 417.
- [37] S. F. Bhat, R. Birkel, D. Wofk, P. Wonka, and M. Müller, "Zoedepth: Zero-shot transfer by combining relative and metric depth," *arXiv preprint arXiv:2302.12288*, 2023.
- [38] W. Yin, C. Zhang, H. Chen, Z. Cai, G. Yu, K. Wang, X. Chen, and C. Shen, "Metric3d: Towards zero-shot metric 3d prediction from a single image," in *ICCV*, 2023.
- [39] Q.-Y. Zhou, J. Park, and V. Koltun, "Open3D: A modern library for 3D data processing," *arXiv:1801.09847*, 2018.
- [40] J. Park, Q.-Y. Zhou, and V. Koltun, "Colored point cloud registration revisited," in *ICCV*, 2017, pp. 143–152.
- [41] C. Doersch, P. Luc, Y. Yang, D. Gokay, S. Koppula, A. Gupta, J. Heyward, I. Rocco, R. Goroshin, J. Carreira, and A. Zisserman, "BootsTAP: Bootstrapped training for tracking-any-point," *ACCV*, 2024.
- [42] X. Lan, Y. Shi, Y. Wu, X. Jiao, and N. Cao, "Kineticharts: Augmenting affective expressiveness of charts in data stories with animation design," *IEEE TVCG*, vol. 28, no. 1, pp. 933–943, 2021.
- [43] P. Sun, H. Kretschmar, X. Dotiwala, A. Chouard, V. Patnaik, P. Tsui, J. Guo, Y. Zhou, Y. Chai, B. Caine et al., "Scalability in perception for autonomous driving: Waymo open dataset," in *CVPR*, 2020, pp. 2446–2454.
- [44] C. Doersch, Y. Yang, M. Vecerik, D. Gokay, A. Gupta, Y. Aytar, J. Carreira, and A. Zisserman, "Tapir: Tracking any point with per-frame initialization and temporal refinement," in *ICCV*, 2023, pp. 10061–10072.
- [45] H. Joo, H. Liu, L. Tan, L. Gui, B. Nabbe, I. Matthews, T. Kanade, S. Nobuhara, and Y. Sheikh, "Panoptic studio: A massively multi-view system for social motion capture," in *ICCV*, 2015, pp. 3334–3342.



Yi He received her B.Eng degree from School of Digital Media & Design Arts, Beijing University of Posts and Telecommunications. She is currently working toward her Ph.D. degree as part of the Intelligent Big Data Visualization (iDV^x) Lab, Tongji University. Her research interests include data visualization and artificial intelligence.



Yuqi Liu received her B.Eng degree from the School of Computer Science and Technology, Shanghai University of Computer Engineering and Science. She is currently working toward her Master's degree as part of the Intelligent Big Data Visualization (iDV^x) Lab at Tongji University. Her research interests include data visualization and artificial intelligence.



Chenpu Li is pursuing his B.Eng dual degree in Visual Communication Design and Artificial Intelligence at the College of Design and Innovation, Tongji University. His current academic focus spans Human-Computer Interaction (CHI) and AI-Art integration.



Ruoyan Chen received her B.Eng degree in Industrial Design from University of Science and Technology Beijing. She is currently pursuing her M.S. degree as part of the Intelligent Big Data Visualization (iDV^x) Lab, Tongji University. Her research interests include data visualization and agent design.



Chuer Chen received her MSc degree from the Department of Electrical and Computer Engineering, National University of Singapore in 2021. She is currently working toward her Ph.D. degree as part of the Intelligent Big Data Visualization (iDV^x) Lab, Tongji University. Her research interests include information visualization and intelligent design.



Shengqi Dang received his B.Sc. in Mathematics from Tongji University and is currently pursuing a Ph.D. degree at the Intelligent Big Data Visualization (iDV^x) Lab, Tongji University. His research interests include artificial intelligence and computer graphics.



Nan Cao received his Ph.D. degree in Computer Science and Engineering from the Hong Kong University of Science and Technology (HKUST), Hong Kong, China in 2012. He is currently a professor at Tongji University and the Assistant Dean of the Tongji College of Design and Innovation. He also directs the Tongji Intelligent Big Data Visualization Lab (iDV^x Lab) and conducts interdisciplinary research across multiple fields, including data visualization, human computer interaction, machine learning, and data mining. He

was a research staff member at the IBM T.J. Watson Research Center, New York, NY, USA before joining the Tongji faculty in 2016.